

Modulation of Endocytic Traffic in Polarized Madin-Darby Canine Kidney Cells by the Small GTPase RhoA

Som-Ming Leung,* Raul Rojas,* Christopher Maples,* Christopher Flynn,* Wily G. Ruiz,* Tzoo-Shuh Jou,[†] and Gerard Apodaca*[‡]

*Renal-Electrolyte Division of the Department of Medicine, Laboratory of Epithelial Biology, and Department of Cell Biology and Physiology, University of Pittsburgh, Pittsburgh, Pennsylvania 15261; and [†]Graduate Institute of Clinical Medicine, College of Medicine, National Taiwan University, Taipei, 100 Taiwan

Submitted June 7, 1999; Accepted September 15, 1999
Monitoring Editor: Suzanne R. Pfeffer

Efficient postendocytic membrane traffic in polarized epithelial cells is thought to be regulated in part by the actin cytoskeleton. RhoA modulates assemblies of actin in the cell, and it has been shown to regulate pinocytosis and phagocytosis; however, its effects on postendocytic traffic are largely unexplored. To this end, we expressed wild-type RhoA (RhoAWT), dominant active RhoA (RhoAV14), and dominant inactive RhoA (RhoAN19) in Madin-Darby canine kidney (MDCK) cells expressing the polymeric immunoglobulin receptor. RhoAV14 expression stimulated the rate of apical and basolateral endocytosis, whereas RhoAN19 expression decreased the rate from both membrane domains. Polarized basolateral recycling of transferrin was disrupted in RhoAV14-expressing cells as a result of increased ligand release at the apical pole of the cell. Degradation of basolaterally internalized epidermal growth factor was slowed in RhoAV14-expressing cells. Although apical recycling of immunoglobulin A (IgA) was largely unaffected in cells expressing RhoAV14, transcytosis of basolaterally internalized IgA was severely impaired. Morphological and biochemical analyses demonstrated that a large proportion of IgA internalized from the basolateral pole of RhoAV14-expressing cells remained within basolateral early endosomes and was slow to exit these compartments. RhoAN19 and RhoAWT expression had little effect on these postendocytic pathways. These results indicate that in polarized MDCK cells activated RhoA may modulate endocytosis from both membrane domains and postendocytic traffic at the basolateral pole of the cell.

INTRODUCTION

Endocytosis comprises a diverse set of mechanisms used by the cell to internalize extracellular fluid as well as small patches of the cell plasma membrane (Mukjherjee *et al.*, 1997). Once internalized, endocytosed fluid and membrane have several postendocytic fates, including return to the cell surface (recycling), delivery to lysosomes, and delivery to the trans-Golgi network (Mukjherjee *et al.*, 1997). In polarized epithelial cells, endocytosis occurs at both the apical and basolateral surfaces of the cell, and internalized macromolecules have the additional option of delivery to the

opposite pole of the cell in a process termed transcytosis (Apodaca *et al.*, 1991). Because of the highly compartmentalized nature of the eukaryotic cell, protein and membrane sorting in these endocytic pathways must be constantly modified during development or in response to changes in the extracellular environment (Mostov and Cardone, 1995).

One mechanism used to regulate endocytic pathways involves changes in the dynamics of the cytoskeleton. Microtubules, for example, are known to be required for transport of contents between early sorting endosomes, late endosomes, and the recycling endosome (Gruenberg *et al.*, 1989; Bomsel *et al.*, 1990; McGraw *et al.*, 1993). In polarized Madin-Darby canine kidney (MDCK) cells, microtubules are necessary for the movement of transcytotic cargo between the basolateral early endosomes and the apical pole of the cell (Breitfeld *et al.*, 1990; Hunziker *et al.*, 1990; Maples *et al.*, 1997). In addition to microtubules, there is increasing evidence that the actin cytoskeleton is required not only for

[‡] Corresponding author. E-mail address: gla6@pitt.edu.
Abbreviations used: DAB, diaminobenzidine; DC, doxycycline; IgA, immunoglobulin A; MDCK, Madin-Darby canine kidney; pIgR, polymeric immunoglobulin receptor; Tf, transferrin; WGA-HRP, wheat germ agglutinin conjugated to HRP.

endocytosis (Gottlieb *et al.*, 1993; Kübler and Riezman, 1993; Jackman *et al.*, 1994; Geli and Riezman, 1996; Lamaze *et al.*, 1997) but also for postendocytic traffic (Durrbach *et al.*, 1996; Maples *et al.*, 1997). We have previously observed that there is a requirement for the actin cytoskeleton early in the transcytotic pathway of polymeric immunoglobulin receptor-immunoglobulin A (pIgR-IgA) complexes (Maples *et al.*, 1997).

The results described above indicate that modulation of the actin cytoskeleton may be an important mechanism for regulating endocytic and postendocytic traffic. One class of macromolecules that couples changes in the external environment to alterations in the actin cytoskeleton is the Rho family of GTPases (Van Aelst and D'Souza-Schorey, 1997; Hall, 1998). This family is composed of at least seven members and their isoforms (Mackay and Hall, 1998): Rho (A, B, and C isoforms), Rac (1 and 2 isoforms), Cdc42 (Cdc42Hs and G25K isoforms), RhoD, RhoG, RhoE, and TC10. One well-known aspect of Rho family function is to regulate the formation of specialized actin structures in the cell. Rac1 directs lamellipodia formation (Ridley *et al.*, 1992), Cdc42 modulates the assembly of filopodia (Kozma *et al.*, 1995), and RhoA controls the formation of stress fibers and focal adhesions (Ridley and Hall, 1992). Further experimentation has revealed that Rho family GTPases control a variety of cellular events, including development, cell growth control, transcription, and membrane trafficking events such as endocytosis (Vojtek and Cooper, 1995; Van Aelst and D'Souza-Schorey, 1997; reviewed by Hall, 1998).

Multiple endocytic pathways are modulated by Rho family members, including phagocytosis (Adam *et al.*, 1996; Chen *et al.*, 1996; Watarai *et al.*, 1997) and pinocytosis (Ridley *et al.*, 1992; Schmalzing *et al.*, 1995). RhoA and Rac1 may also be important regulators of receptor-mediated endocytosis. Dominant active mutants of these proteins inhibit endocytosis of transferrin receptor in intact as well as perforated cells (Lamaze *et al.*, 1996). We have recently observed that Rac1 modulates endocytosis from both the basolateral and apical poles of MDCK cells (Jou *et al.*, 2000). In addition, a dominant active mutant of Rac1 (Rac1V12) selectively alters apically directed postendocytic traffic, including apical recycling and basolateral-to-apical transcytosis (Jou *et al.*, 2000). Recent evidence indicates that Cdc42 may be important in regulating the delivery of newly synthesized proteins to the basolateral domain of MDCK cells (Kroschewski *et al.*, 1999). Although the role of RhoB in endocytic traffic is not established, it has been localized to early endosomes and synaptic microvesicles (Adamson *et al.*, 1992; Cussac *et al.*, 1996). RhoD, a recently described member of the Rho family, is found on early endosomes as well as on the plasma membrane (Murphy *et al.*, 1996). Overexpression of dominant active RhoD causes endosomal scattering, and in time-lapse video microscopy endosomes are observed to have decreased motility (Murphy *et al.*, 1996).

We analyzed endocytic traffic in MDCK cells expressing mutant and wild-type RhoA (RhoAWT). We find that RhoA regulates the rate of endocytosis at both poles of polarized MDCK cells. In addition, expression of dominant active RhoA (RhoAV14) dramatically slows basolateral-to-apical transcytosis of pIgR-IgA as a result of the trapping of ligand in basal endosomes. Although basolateral recycling of transferrin (Tf) was slowed, apical recycling of IgA was unaf-

ected. This analysis reveals previously undescribed functions for activated RhoA in regulating endocytic rates at both cell surfaces and postendocytic traffic at the basolateral pole of the MDCK cell.

MATERIALS AND METHODS

Generation of Cell Lines Expressing Wild-Type and Mutant RhoA

pEXV-myc-RhoAWT and pEXV-myc-RhoAV14 cDNAs were generously provided by Dr. A. Hall (MRC Laboratory of Molecular Cell Biology, London, United Kingdom) (Ridley and Hall, 1992). The vectors were digested with *EcoRI* to remove the insert containing myc-RhoAWT or myc-RhoAV14 DNA and then ligated into *EcoRI*-digested and dephosphorylated pTRE vector (Clontech, Palo Alto, CA). *Escherichia coli* was transfected with the vector constructs and selected for ampicillin resistance. Plasmid DNAs were purified from bacterial cells expressing pTRE-myc-RhoAWT or pTRE-myc-RhoAV14 cDNAs in the appropriate orientation (assessed by DNA sequencing). The T23 clone of MDCK cells (which express a tetracycline-repressible transactivator and the pIgR) (Barth *et al.*, 1997) was cotransfected with 20 μ g of pTRE-myc-RhoAWT or pTRE-myc-RhoAV14 and 2 μ g of the pCB7 vector that contains a hygromycin resistance gene with the use of CaPO₄ precipitation, as described previously (Breitfeld *et al.*, 1989a). After 2–3 d of incubation in the presence of 20 ng/ml doxycycline (DC) (Sigma, St. Louis, MO), the cells were diluted into selection medium containing minimal essential medium (MEM), 10% (vol/vol) FBS, 250 μ g/ml hygromycin, and 20 ng/ml DC. The DC stock solution (20 μ g/ml in 95% ethanol) was stored at -20°C and was diluted 1:1000 just before use. After selection for 10 d, surviving colonies were isolated with the use of cloning rings, and RhoAWT or RhoAV14 expression was assessed by Western blotting and immunofluorescence 36 h after removal of DC. Positive clones were expanded in the presence of DC, divided into aliquots, and stored in liquid nitrogen. Several clones of each type were selected and then screened for polarized secretion of GP-80 (Urban *et al.*, 1987) and a transepithelial resistance of $>120 \Omega/\text{cm}^2$ when cultured on Transwells (Corning-Costar, Cambridge, MA) in the presence of 20 ng/ml DC. The data presented are from an individual, representative clone that uniformly expressed high levels of either myc-RhoAWT or myc-RhoAV14 when cells were cultured in the absence of DC. However, similar results were obtained with other clones expressing these mutant proteins. T23 MDCK cells expressing dominant negative myc-tagged RhoAN19 have been described previously (Jou and Nelson, 1998).

Cell Culture

The cell lines were routinely cultured in MEM/FBS containing 10% (vol/vol) FBS, penicillin/streptomycin/Fungizone, and 20 ng/ml DC at 37°C in a humidified atmosphere containing 5% CO₂. Expression of RhoAWT, RhoAV14, or RhoAN19 was induced by plating cells in 15-cm dishes at low density into MEM/FBS medium containing 0–5 pg/ml DC and incubating them for 36–48 h at 37°C . At the end of this incubation period, the cells had reached $\sim 30\%$ confluence. Cells treated in an identical manner, but in the presence of 20 ng/ml DC, served as controls. The cells were trypsinized and washed with culture medium containing 5 μM calcium chloride (LCM), and 1×10^6 cells (resuspended in 0.5 ml of LCM) were added to the apical chamber of rat tail, collagen-coated, 12-mm-diameter Transwells in LCM containing either 20 ng/ml DC (control) or 0–5 pg/ml DC. Cells were incubated in LCM for 3–4 h (with or without DC), rinsed twice with PBS, and then incubated in MEM/FBS containing either 20 ng/ml DC (control) or 0–5 pg/ml DC and normal amounts of LCM (1.8 mM) for 18–48 h.

Antibodies, Proteins, and Other Markers

The following reagents were used: mouse anti-myc hybridoma 9E10 ascites (Dr. S.W. Whiteheart, University of Kentucky, Lexington, KY); rat anti-ZO-1 hybridoma R40.76 ascites (Dr. D.A. Goodenough, Harvard University, Cambridge, MA); purified mouse anti-RhoA mAb (Santa Cruz Biotechnology, Santa Cruz, CA); affinity-purified rabbit polyclonal anti-human IgA antibody (Jackson Immunoresearch Laboratories, West Grove, PA); affinity-purified and minimal cross-reacting fluorescein- and Cy5-conjugated secondary antibodies (Jackson Immunoresearch Laboratories); human polymeric IgA (Dr. K. Mostov, University of California, San Francisco, CA); and FITC-phalloidin (Molecular Probes, Eugene, OR).

Western Blot Analysis

Western blot analysis was performed as described previously (Maples *et al.*, 1997).

Immunofluorescent Labeling and Scanning Laser Confocal Microscopy

Cells were fixed and processed with a pH shift protocol (Apodaca *et al.*, 1994). Imaging was performed on a TCS confocal microscope equipped with krypton, argon, and helium-neon lasers (Leica, Deerfield, IL). Images were acquired with the use of a 100 \times plan-apochromat objective (numerical aperture, 1.4) and the appropriate filter combination. Settings were as follows: photomultipliers set to 600–800 mV, 1.5- μ m pinhole, zoom = 2.0–3.0, Kalman filter ($n = 4$). The images (1024 \times 1024 pixels) were saved in tag-information-file format, and the contrast levels of the images were adjusted in Photoshop (Adobe, Mountain View, CA) on a Power PC G-3 Macintosh computer (Apple, Cupertino, CA). The contrast-corrected images were imported into Freehand (Macromedia, San Francisco, CA) and printed from a Kodak (Rochester, NY) 8650PS dye sublimation printer.

Endocytosis of [¹²⁵I]IgA

Endocytosis of [¹²⁵I]IgA was measured as described (Apodaca *et al.*, 1994). Values for endocytosed ligand from filters that were never warmed to 37°C (typically <5% of the total bound counts) were subtracted from the endocytosis values of cells that were allowed to internalize ligand at 37°C.

Measurement of Paracellular Diffusion of [¹²⁵I]IgA and [¹²⁵I]Tf

Filter-grown cells were washed three times with MEM/BSA and [¹²⁵I]IgA or [¹²⁵I]Tf, diluted in 0.5 ml of MEM/BSA containing a 100-fold excess of unlabeled IgA or Tf, and added to the apical chamber of the Transwell. Cold competing ligand was added to prevent receptor-mediated internalization and apical-to-basolateral transcytosis. MEM/BSA (0.5 ml) was placed in the basolateral chamber. At the designated times, the basolateral MEM/BSA (0.5 ml) was collected and replaced with fresh MEM/BSA. After the final time point, filters were washed twice with ice-cold PBS and cut out of the insert, and the amount of [¹²⁵I]IgA or [¹²⁵I]Tf that remained in the apical medium, that had diffused into the basolateral chamber, or that remained cell associated was quantified in a gamma counter. The results are expressed as the percentage of [¹²⁵I]IgA or [¹²⁵I]Tf initially added to the apical chamber that was released basolaterally.

Analysis of the Postendocytotic Fate of [¹²⁵I]IgA

The postendocytotic fate of a preinternalized cohort of [¹²⁵I]IgA (at 5–10 μ g/ml) was analyzed as described (Apodaca *et al.*, 1994; Maples *et al.*, 1997). In preliminary experiments, we performed assays in the presence of a 100-fold excess of cold competing IgA.

Because the amount of fluid-phase internalization was <5% of the signal observed in pIgR-expressing cells, this step was omitted in subsequent experiments.

Analysis of [¹²⁵I]Tf Recycling

Iron-saturated Tf was iodinated to a specific activity of 5.0–9.0 $\times 10^6$ cpm/ μ g with the use of ICl as described (Apodaca *et al.*, 1994; Maples *et al.*, 1997). The cells were washed with warm (37°C) MEM/BSA three times, and unlabeled Tf was allowed to dissociate from the cell surface and filter for 60 min in MEM/BSA. [¹²⁵I]Tf (5 μ g/ml) was internalized from the basolateral surface of the cells for 45 min at 37°C in a humid chamber. The cells were washed three times for 5 min each with ice-cold MEM/BSA and then warmed to 37°C for 2.5 min to allow for receptor internalization, as described previously (Apodaca *et al.*, 1994; Maples *et al.*, 1997). The medium was aspirated, fresh medium was added, and the postendocytotic fate of [¹²⁵I]Tf was assessed as described above. [¹²⁵I]Tf uptake was inhibited >95% when the radioactive ligand was internalized in the presence of a 100-fold excess of cold ligand.

Analysis of [¹²⁵I]EGF Degradation

[¹²⁵I]EGF (150–200 μ Ci/ μ g) was purchased from New England Nuclear (Boston, MA) and used at a final concentration of 40 ng/ml. The cells were washed with warm (37°C) MEM/BSA three times, and [¹²⁵I]EGF was internalized from the basolateral surface of the cells for 10 min at 37°C. The cells were washed rapidly three times with MEM/BSA, the apical and basolateral media were aspirated and replaced with fresh MEM/BSA, and the cells were then incubated for 3 min at 37°C. The medium was aspirated, fresh medium was added, and the postendocytotic fate of [¹²⁵I]EGF was assessed and trichloroacetic acid precipitations of media samples were performed as described above.

Diaminobenzidine Density-Shift Assay

We have used a modified version of the diaminobenzidine (DAB) density-shift assay described previously (Apodaca *et al.*, 1994, 1996). [¹²⁵I]IgA (5 μ g/ml) was internalized basolaterally, and 25–50 μ g/ml wheat germ agglutinin conjugated to HRP (WGA-HRP) (Vector Laboratories, Burlingame, CA) was cointernalized from the apical pole of the cells. The concentration of WGA-HRP was adjusted so that equivalent amounts of WGA-HRP were internalized by control and RhoA14-expressing cells. After internalization, the cells were washed with ice-cold MEM/BSA. [¹²⁵I]IgA was stripped from the basolateral cell surface with 100 μ g/ml trypsin (diluted in MEM/BSA) for 3 \times 10 min at 4°C, and cell surface WGA-HRP was simultaneously removed by treating the apical cell surface for 3 \times 10 min with 100 mM *N*-acetyl-D-glucosamine (dissolved in MEM/BSA). The cells were then washed twice with ice-cold 200 mM sodium cacodylate buffer, pH 7.4, and DAB reaction buffer (0.5 ml) was added to both apical and basal compartments of the Transwell. DAB reaction buffer was prepared by adding 40 mg of DAB to 40 ml of H₂O and then adding 1.8 g of solid sodium cacodylate. The buffer was adjusted to pH 7.4 with NaOH and filtered, and 1 μ l of 30% (vol/vol) H₂O₂ was added for each milliliter of DAB reaction buffer. In control reactions, H₂O₂ was omitted from the DAB reaction buffer. After a 45-min incubation at 4°C, the cells were washed two times with 200 mM sodium cacodylate buffer, and the filters were carefully excised from their holders, boiled in 0.4 ml of SDS lysis buffer (0.5% [wt/vol] SDS, 100 mM triethanolamine, pH 8.6, 5 mM EDTA, 0.02% [wt/vol] NaN₃) for 90 s, and vortex shaken for 15 min at 4°C. Under these conditions, <5% of the total radioactivity was associated with the filter. The supernatants were then centrifuged at 100,000 \times g in a RP70AT rotor (Sorvall, Wilmington, DE) for 30 min at 20°C in a RCM100 centrifuge (Sorvall). Radioactivity present in the pellet and supernatant was quantified in a gamma counter. Values were normalized to reactions in which [¹²⁵I]IgA and WGA-

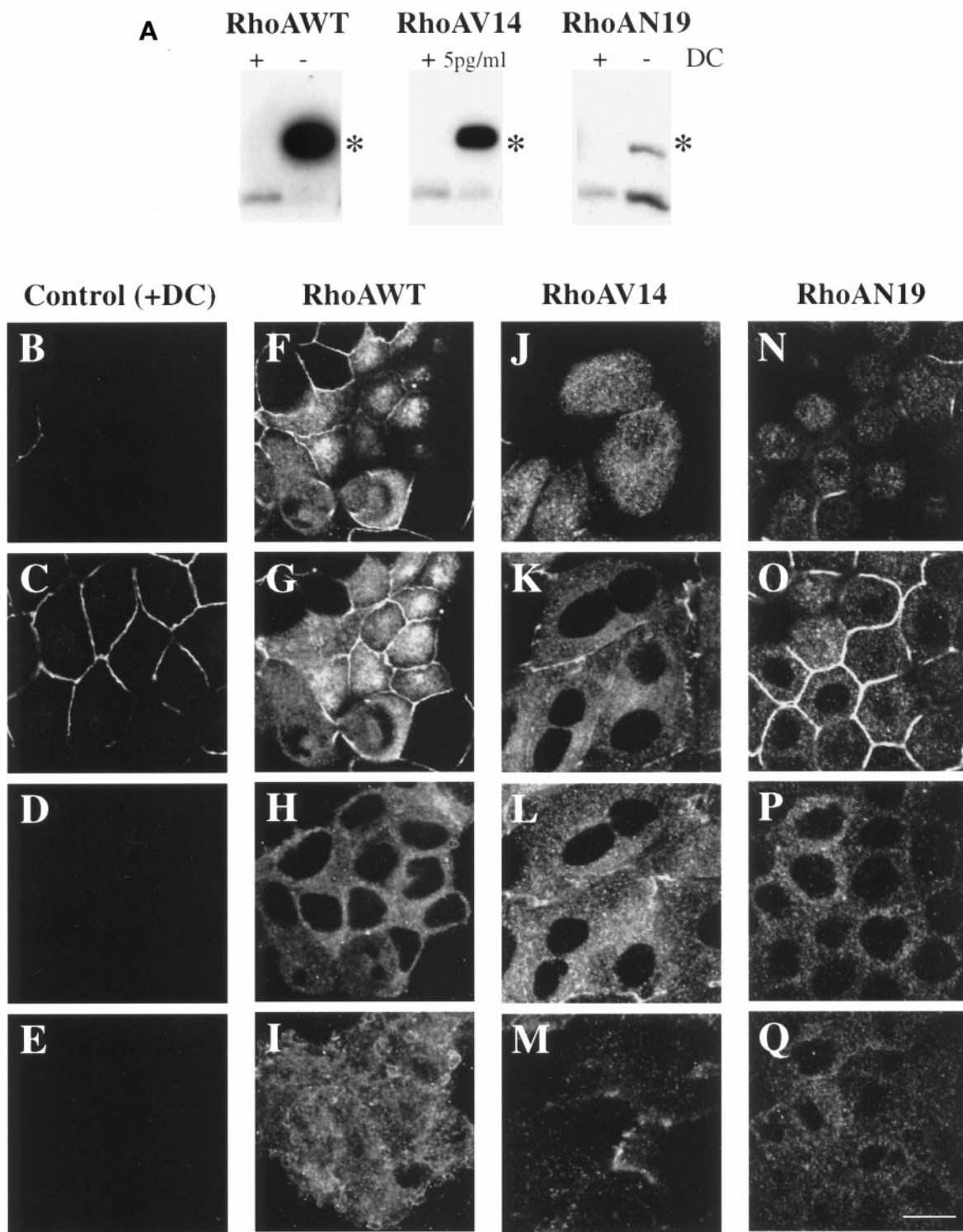


Figure 1. Inducible expression and distribution of myc-tagged RhoAWT, RhoAV14, and RhoAN19 in polarized MDCK cells. (A) RhoAWT, RhoAV14, and RhoAN19 cells were plated at low density in medium containing 0–5 pg/ml DC (– or 5pg/ml) or containing 20 ng/ml DC (+), incubated for 36–48 h, and then plated on Transwell filter supports (with or without DC). After 18 h, the filter-grown cells were solubilized in SDS lysis buffer, 10 μ g of lysate was resolved by PAGE, and Western blots were probed with an anti-RhoA mAb to detect induction of the myc-tagged mutant proteins as well as endogenous RhoA. Asterisks indicate that the addition of the myc tag to RhoAWT, RhoAV14, and RhoAN17 causes these proteins to migrate slower than endogenous RhoA. (B–Q) Distribution of ZO-1 and myc-tagged

HRP were cointernalized from the apical pole of the cell, as described previously (Apodaca *et al.*, 1994, 1996).

RESULTS

Induction of RhoA Overexpression in Polarized MDCK Cells

We used the T23 clone of MDCK cells that stably expresses the tetracycline transactivator (Barth *et al.*, 1997) and NH₂-terminal myc-tagged RhoAWT, dominant active RhoAV14, or dominant inactive RhoAN19. These cells also express pIgR. The level of expression of wild-type and mutant RhoA was regulated by the addition of DC. In the presence of 20 ng/ml DC, expression of neither wild-type nor mutant RhoA was detected by Western blotting (Figure 1A), nor was expression detected by immunofluorescence with the 9E10 mAb that specifically recognizes the myc tag (Figure 1, B–E). The data shown in Figure 1, B–E, are for RhoAV14 cells grown in the presence of 20 ng/ml DC. Identical results were obtained with RhoAWT and RhoAN19 cells grown in the presence of 20 ng/ml DC.

The tetracycline-repressible system allows the level of transgene expression to be regulated by altering the amount of DC added to the cell cultures. When RhoAWT cells were cultured on Transwells in the absence of DC for 18 h, the amount of RhoAWT was determined to be ~12-fold greater than the level of endogenous RhoA (Figure 1A). A similar level of expression was observed 48 h after plating on Transwells. When examined by immunofluorescence, myc-tagged RhoAWT was distributed throughout the cell in a diffuse cytoplasmic staining pattern as well as in punctate structures (Figure 1, F–I). We costained the cells for the tight junction-associated protein ZO-1, because this structure serves as a convenient landmark to identify the border between the apical and basolateral plasma membrane domains. Moreover, it has been shown that tight junction morphology and function are altered in cells expressing mutants of RhoA (Jou *et al.*, 1998). ZO-1 staining in RhoAWT-expressing cells was similar to that observed in control cells (Figure 1, compare C and G; ZO-1 is the thin bright line that surrounds each cell).

Because expression of RhoAV14 has dramatic consequences on the tight junction function and the integrity of cell monolayers (Jou *et al.*, 1998), we determined in a preliminary set of experiments that derepression of RhoAV14 transcription in the presence of 5 pg/ml DC allowed for an ~10.6-fold level of overexpression (Figure 1A) while main-

taining an acceptable level of barrier function (see below). Similar levels of expression were observed 48 h after plating on Transwells. The distribution of RhoAV14 was cytosolic or punctate in appearance (Figure 1, J–M). The punctate structures at the base of the cell are apparently endocytic in nature (see Figure 8). As described previously (Jou *et al.*, 1998), ZO-1 staining was irregular and penetrated to the lateral membranes of the cell (Figure 1, J–L).

The amount of RhoAN19 expression was ~40% of the level of endogenous RhoA 18 h after plating on Transwells and was similar to the level of expression described previously (Jou and Nelson, 1998). This level of overexpression was maintained for up to 48 h after plating on Transwells. Although this level was much less than that obtained for RhoAWT and RhoAV14, we were unable, after several attempts, to obtain stably transfected cells that had higher levels of expression (see also Takaishi *et al.*, 1997; Jou and Nelson, 1998). The distribution of myc-tagged RhoAN19 and ZO-1 was similar to the myc-tagged wild-type RhoA and ZO-1 staining observed in RhoAWT cells (Figure 1, N–Q).

In biochemical experiments described below, we used RhoAWT, RhoAV14, or RhoAN19 cells 18–48 h after plating and obtained similar results. It has been observed that at these times polarized trafficking of proteins occurs to both the apical and basolateral membrane domains (Grindstaff *et al.*, 1998).

Apical and Basolateral Endocytosis Is Altered by Mutant RhoA Expression

To determine whether RhoA regulated endocytosis in MDCK cells, we measured the internalization of [¹²⁵I]IgA from either the apical or the basolateral pole of cells expressing RhoAWT, RhoAV14, or RhoAN19. RhoAWT expression had no clear-cut effect on either apical (Figure 2A) or basolateral (Figure 2B) endocytosis. In cells expressing RhoAV14, the rate and extent of both apical and basolateral endocytosis were significantly stimulated by expression of dominant active RhoAV14 protein (Figure 2, C and D). The effect was especially pronounced at the apical pole of the cell, where endocytosis was stimulated approximately twofold at each time point relative to control. In contrast, both the rate and the extent of apical and basolateral endocytosis was decreased by RhoAN19 expression (Figure 2, E and F). The significant decrease (~25–50%) in apical endocytosis was observed at the 1- and 7.5-min time points. A decrease (~25–40%) in basolateral endocytosis was apparent at all time points. In summary, the results indicate that in polarized MDCK cells, endocytosis may be modulated by RhoA; activation of RhoA increases the rate of endocytosis, whereas inactivation of RhoA decreases the rate of endocytosis.

Postendocytic Traffic Is Altered in RhoAV14-expressing Cells

Previously, we observed that efficient postendocytic traffic requires an intact actin cytoskeleton (Maples *et al.*, 1997). Therefore, we next explored the effect of RhoAWT, RhoAV14, or RhoAN19 expression on these pathways. We followed markers of the basolateral recycling pathway, the apical recycling pathway, the degradative pathway, or the basolateral-to-apical transcytotic pathway. As described

Figure 1 (cont). proteins in RhoAV14 cells grown in the presence of 20 ng/ml DC (B–E), RhoAWT cells grown in the absence of DC (F–I), RhoAV14 cells grown in the presence of 5 pg/ml DC (J–M), or RhoAN19 cells grown in the absence of DC (N–Q). Cells were fixed with paraformaldehyde and stained with antibodies that recognize the tight junction protein ZO-1 or the myc tag, and emission from FITC-conjugated secondary antibodies was captured with the use of a scanning laser confocal microscope. Shown are optical sections from the base of the cells (E, I, M, and Q), along the lateral surface of the cells (D, H, L, and P), at the level of the tight junctions (C, G, K, and O), and at the very apex of the cells (B, F, J, and N). The tight junctions are the thin, brightly stained lines that surround each cell. IgA was internalized at the basolateral pole of these cells, but staining for this marker is not shown. Bar, 10 μm.

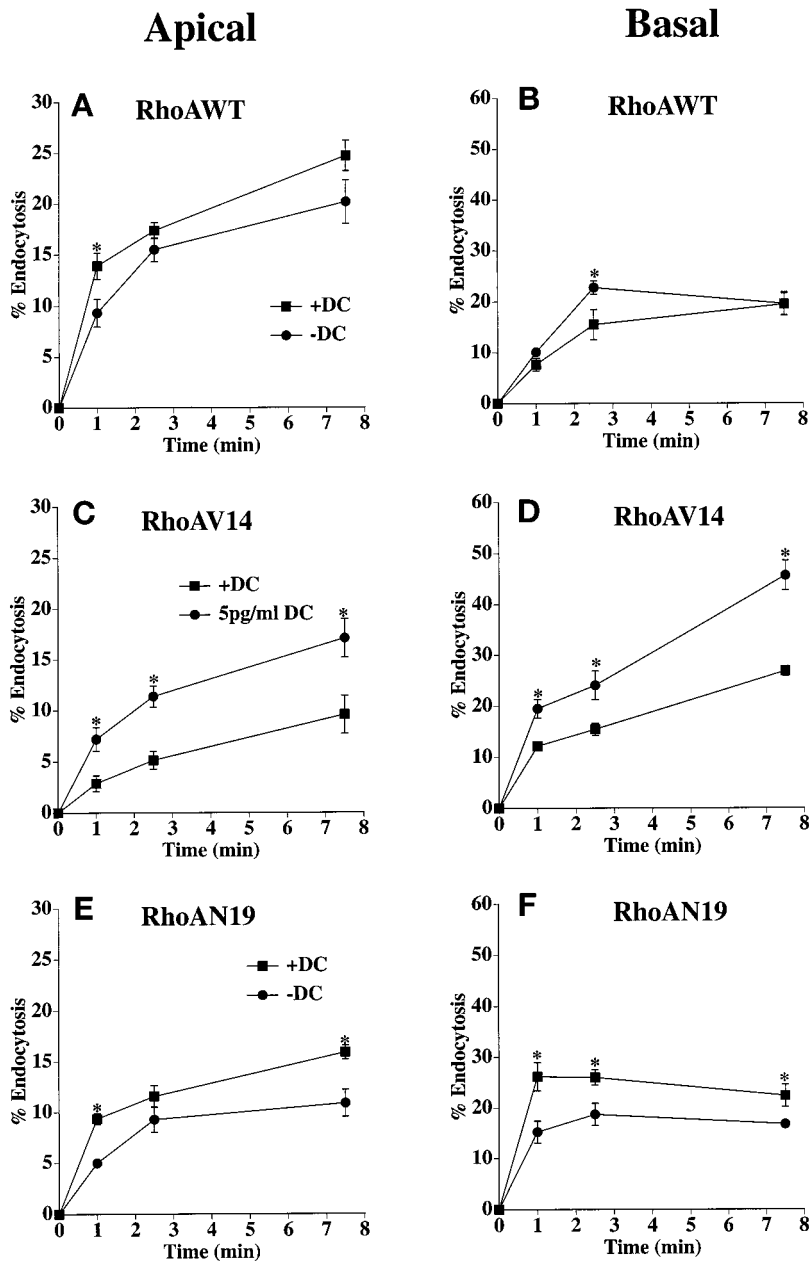


Figure 2. Apical and basolateral endocytosis in RhoAWT, RhoAV14, or RhoAN19 cells. [125 I]IgA was bound to the apical (A, C, and E) or basolateral (B, D, and F) surface of the cells for 60 min at 4°C. The RhoAWT (A and B), RhoAV14 (C and D), or RhoAN19 (E and F) cells, cultured in the presence of 20 ng/ml DC (+DC) or 0–5 pg/ml DC (–DC or 5pg/ml DC), were washed and then incubated at 37°C for the times indicated. Medium was collected, and the cells were then rapidly cooled on ice. [125 I]IgA was stripped from the cell surface by a sequential treatment of trypsin and acid at 4°C, and the filters were then cut out of their holders. Total [125 I]IgA initially bound to the cells included ligand released into the medium, ligand stripped from the cell surface with trypsin and acid, and cell-associated ligand not sensitive to stripping (endocytosed). Shown is the percentage of total ligand endocytosed (mean \pm SEM; $n \geq 4$). Statistical significance was assessed with the use of a *t* test. Values for which $p < 0.05$ are marked with asterisks. Endocytosis values from filters that were never warmed to 37°C were subtracted from the endocytosis values of cells that were allowed to internalize ligand at 37°C.

above and reported previously, cells expressing RhoAV14 and RhoAN19 have disrupted tight junctions with altered “gate” and “fence” functions (Jou *et al.*, 1998). In the assays described below, we measured the movement of ligand between the apical and basolateral compartments of the Transwell. Because large-scale diffusion of ligands would significantly alter the interpretation of the results, we determined the extent of [125 I]IgA and [125 I]Tf flux in cells expressing wild-type and mutant RhoA. Less than 0.5% of apically added [125 I]IgA or [125 I]Tf appeared in the basolateral compartments of RhoAWT, RhoAV14, or RhoAN19 cells after 60 min at 37°C (our unpublished results). We

deemed this small increase in flux insufficient to alter the outcome of the postendocytic fate assays described below.

We used Tf as a marker of the basolateral recycling pathway. In control cells, Tf is internalized almost exclusively from the basolateral pole of the cell and rapidly recycles back to this cell surface (Fuller and Simons, 1986). Recycling of basolaterally internalized [125 I]Tf was not significantly altered in cells expressing RhoAWT (Figure 3A). However, Tf recycling was significantly slowed in cells expressing RhoAV14 (Figure 3B). This decrease was coupled with an increase in the amount of ligand released from the apical pole of the cell (~10% in control cells versus ~30% in cells

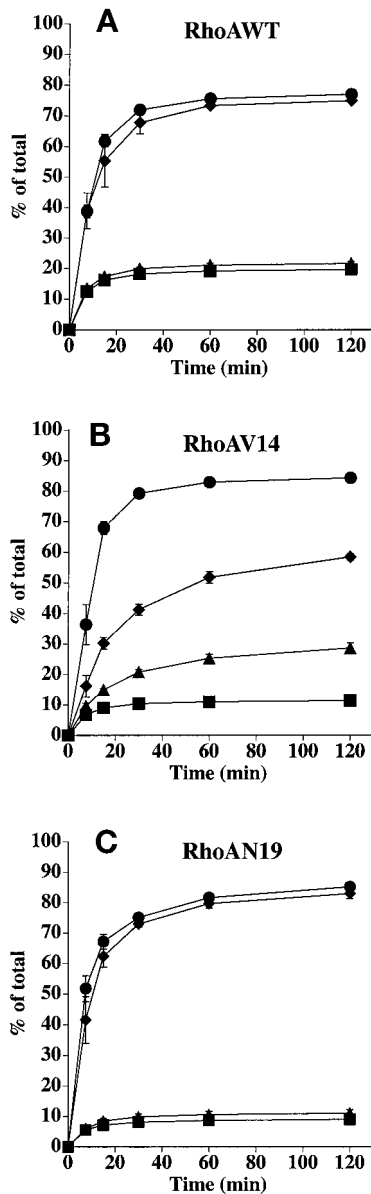


Figure 3. Postendocytic fate of basolaterally internalized Tf in RhoAWT, RhoAV14, or RhoAN19 cells. [125 I]Tf was internalized from the basolateral pole of the cell for 45 min at 37°C. The cells were then washed at 4°C and warmed for 2.5 min at 37°C to allow for receptor internalization, and the postendocytic fate of internalized [125 I]Tf was determined in a 120-min chase at 37°C. The percentage of ligand released basolaterally (recycled) or released apically (transcytosed) in RhoAWT (A), RhoAV14 (B), or RhoAN19 (C) cells is shown. Values for degradation were as follows: RhoAWT + DC, $1.9 \pm 0.2\%$; RhoAWT - DC, $1.9 \pm 0.1\%$; RhoAV14 + DC, $1.9 \pm 0.4\%$; RhoAV14 + 5 pg/ml DC, $2.6 \pm 0.2\%$; RhoAN19 + DC, $2.6 \pm 0.3\%$; RhoAN19 - DC, $3.0 \pm 0.2\%$. Values for ligand remaining cell associated were as follows: RhoAWT + DC, $1.5 \pm 0.2\%$; RhoAWT - DC, $1.4 \pm 0.1\%$; RhoAV14 + DC, $2.3 \pm 0.5\%$; RhoAV14 + 5 pg/ml DC, $10.3 \pm 2.1\%$; RhoAN19 + DC, $3.1 \pm 0.3\%$; RhoAN19 - DC, $3.0 \pm 0.8\%$. Values (mean \pm SD; n = 3) are from a representative experiment. (A and C) ■, +DC, transcytosed; ●, +DC, recycled; ▲, -DC, transcytosed; ◆, -DC, recycled. (B) ■, +DC, transcytosed; ●, +DC, recycled; ▲, 5 pg/ml DC, transcytosed; ◆, 5 pg/ml DC, recycled.

expressing RhoAV14). There was little difference in the amount of [125 I]Tf degraded ($\sim 2\text{--}3\%$), but there was a small increase in the amount of ligand that remained cell associated ($\sim 2\%$ in control cells versus $\sim 10\%$ in RhoAV14 expressors). There was only a slight effect of RhoAN19 expression on polarized Tf traffic (Figure 3C). These observations indicate that RhoAV14 expression alters the efficient sorting of Tf into the basolateral recycling pathway of polarized MDCK cells.

EGF is primarily delivered to late endosomes/lysosomes, where it is degraded (reviewed by Mukjherjee *et al.*, 1997; Schmid, 1997). In MDCK cells, a fraction of the ligand ($\sim 20\text{--}25\%$) also recycles at the basolateral pole of the cell or is released at the apical pole of the cell ($\sim 5\text{--}10\%$) (Brandli *et al.*, 1991). The majority of [125 I]EGF internalized from the basolateral surface of cells expressing RhoAWT was degraded ($\sim 60\%$) (Figure 4A), $\sim 20\%$ was recycled to the basolateral surface, $\sim 10\%$ was transcytosed, and the balance remained cell associated. RhoAV14 expression slowed the degradation of [125 I]EGF (Figure 4B) and reduced the maximal levels of degradation by $\sim 15\%$. There was no significant effect on the amount of ligand released at the apical or the basolateral pole of the cell, but the amount of ligand that remained cell associated was increased from 3% in control cells to 7% in RhoAV14-expressing cells. RhoAN19 expression did not affect EGF degradation (Figure 4C).

IgA internalized from the apical pole of pIgR-expressing cells was used as a marker of the apical recycling pathway. Although pIgR normally moves by transcytosis from the basolateral to the apical pole of the cell, where it is cleaved to the secretory component (Apodaca *et al.*, 1991), a fraction of the receptor escapes cleavage and can be internalized from the apical cell surface (Breitfeld *et al.*, 1989b). This apically internalized pool of IgA primarily recycles to the apical membrane (Apodaca *et al.*, 1994). In cells expressing RhoAWT, the majority of apically internalized ligand was rapidly recycled to the apical pole of the cell, and there was no difference between RhoAWT cells grown in the presence or absence of DC (Figure 5A). In RhoAV14-expressing cells, there was a small increase in the kinetics of apical recycling versus control cells, but there was no effect on the extent of IgA recycling (Figure 5B). Compared with control cells, there was no difference in the amount of ligand that was degraded ($\sim 5\%$) or remained cell associated ($\sim 7\%$) in RhoAV14-expressing cells. Finally, RhoAN19 expression increased the kinetics of apical [125 I]IgA recycling in a reproducible manner. No effect on degradation was observed, but there was a small decrease in the amount of cell-associated ligand ($\sim 9\%$ in control cells versus $\sim 4\%$ in RhoAN19-expressing cells).

Next, we measured the effect of wild-type and mutant RhoA expression on the postendocytic fate of basolaterally internalized [125 I]IgA. When internalized basolaterally, pIgR-IgA complexes move sequentially between basolateral early endosomes, a common endosomal compartment, and the apical recycling endosome before release at the apical pole of the cell (Apodaca *et al.*, 1994; Odorizzi *et al.*, 1996). There was little effect of RhoAWT expression on the postendocytic fate of basolaterally internalized IgA (Figure 6A). In contrast, in cells expressing RhoAV14 there was a significant slowing of basolateral-to-apical transcytosis (Figure 6B); transcytosis was inhibited by $\sim 70\%$. This inhibition of trans-

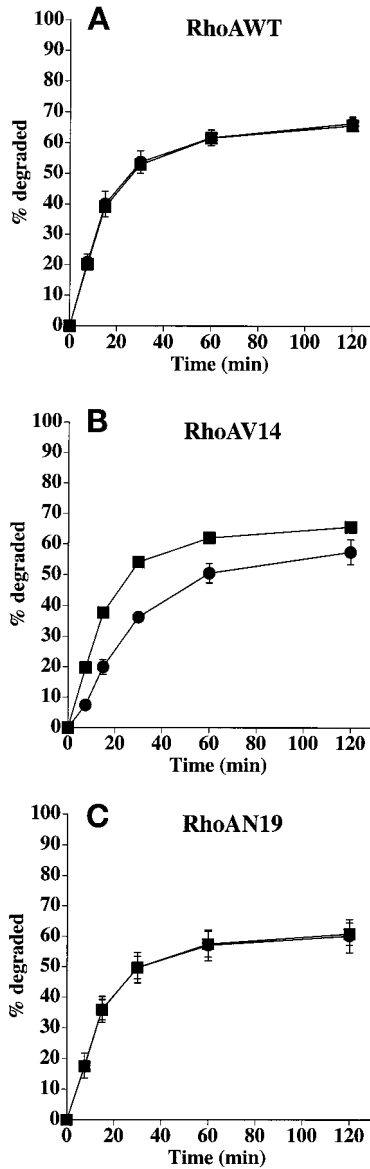


Figure 4. Postendocytic fate of basolaterally internalized EGF in RhoAWT, RhoAV14, or RhoAN19 cells. [¹²⁵I]EGF was internalized from the basolateral surface of cells for 10 min at 37°C, and the cells were quickly washed and then chased for 120 min. The percentage of total degraded ligand released from RhoAWT (A), RhoAV14 (B), or RhoAN19 (C) cells is shown. Values for transcytosis were as follows: RhoAWT + DC, 10.1 ± 0.4%; RhoAWT - DC, 11.1 ± 1.0%; RhoAV14 + DC, 9.0 ± 1.0%; RhoAV14 + 5 pg/ml DC, 11.5 ± 2.3%; RhoAN19 + DC, 9.2 ± 0.7%; RhoAN19 - DC, 12.5 ± 3.3%. Values for ligand recycling were as follows: RhoAWT + DC, 19.4 ± 1.2%; RhoAWT - DC, 17.9 ± 1.3%; RhoAV14 + DC, 22.7 ± 0.5%; RhoAV14 + 5 pg/ml DC, 24.6 ± 2.8%; RhoAN19 + DC, 16.8 ± 0.7%; RhoAN19 - DC, 17.1 ± 0.9%. Values for ligand remaining cell associated were as follows: RhoAWT + DC, 5.0 ± 0.8%; RhoAWT - DC, 4.8 ± 0.3%; RhoAV14 + DC, 2.8 ± 0.5%; RhoAV14 + 5 pg/ml DC, 6.6 ± 1.2%; RhoAN19 + DC, 13.2 ± 5.1%; RhoAN19 - DC, 10.3 ± 3.0%. Values (mean ± SD; n = 3) are from a representative experiment. (A and C) ■, +DC; ●, -DC. (B) ■, +DC; ●, 5 pg/ml DC.

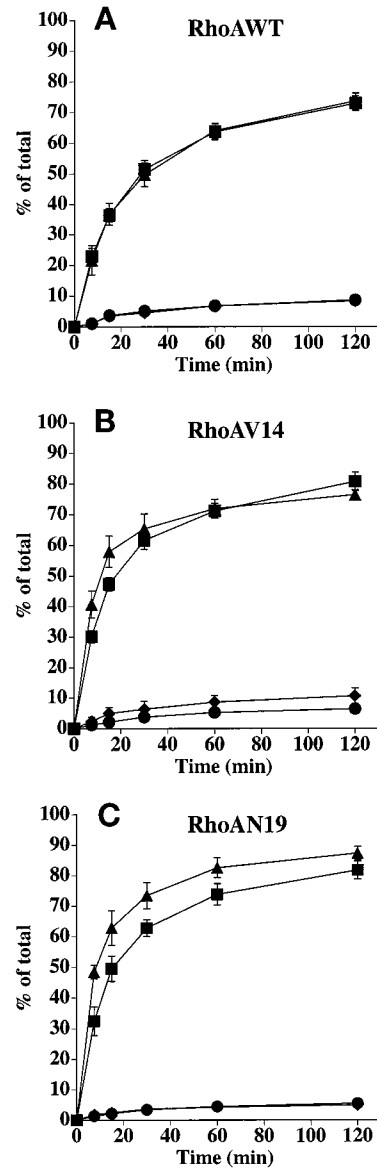


Figure 5. Postendocytic fate of apically internalized IgA in RhoAWT, RhoAV14, or RhoAN19 cells. [¹²⁵I]IgA was internalized from the apical surface of cells for 10 min at 37°C, and the cells were quickly washed and then chased for 120 min. The percentage of total ligand released apically (recycled) or basolaterally (transcytosed) in RhoAWT (A), RhoAV14 (B), or RhoAN19 (C) cells is shown. Values for degradation were as follows: RhoAWT + DC, 5.9 ± 0.5%; RhoAWT - DC, 5.3 ± 0.3%; RhoAV14 + DC, 5.0 ± 0.8%; RhoAV14 + 5 pg/ml DC, 5.7 ± 1.3%; RhoAN19 + DC, 4.2 ± 0.8%; RhoAN19 - DC, 3.5 ± 1.6%. Values for ligand remaining cell associated were as follows: RhoAWT + DC, 12.6 ± 2.1%; RhoAWT - DC, 12.7 ± 1.3%; RhoAV14 + DC, 7.9 ± 2.0%; RhoAV14 + 5 pg/ml DC, 7.3 ± 0.3%; RhoAN19 + DC, 8.5 ± 1.9%; RhoAN19 - DC, 4.2 ± 0.5%. Values (mean ± SD; n = 3) are from a representative experiment. (A and C) ■, +DC, recycled; ●, +DC, transcytosed; ▲, -DC, recycled; ◆, -DC, transcytosed. (B) ■, +DC, recycled; ●, +DC, transcytosed; ▲, 5 pg/ml DC, recycled; ◆, 5 pg/ml DC, transcytosed.

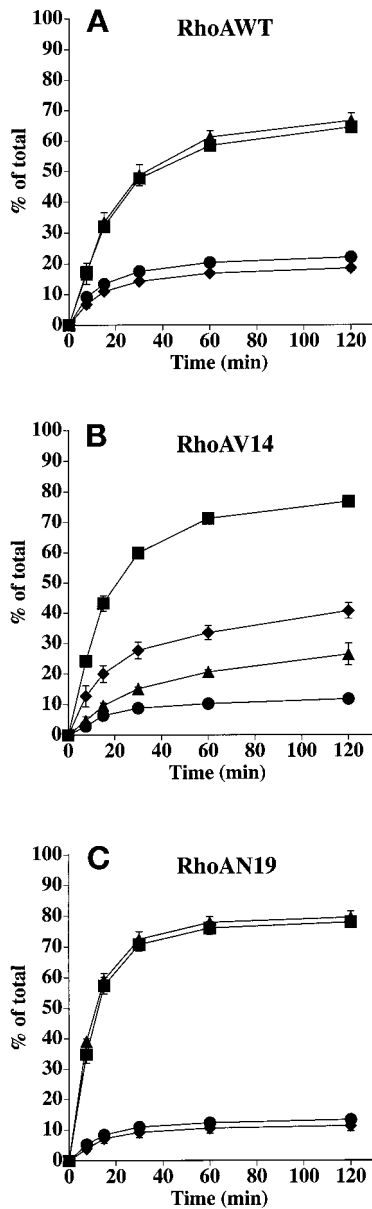


Figure 6. Postendocytic fate of basolaterally internalized IgA in RhoAWT, RhoAV14, or RhoAN19 cells. [125 I]IgA was internalized from the basolateral surface of cells for 5 min at 37°C, and the cells were quickly washed and then chased for 120 min. The percentage of total ligand released basolaterally (recycled) or apically (transcytosed) in RhoAWT (A), RhoAV14 (B), or RhoAN19 (C) cells is shown. Values for degradation were as follows: RhoAWT + DC, $5.3 \pm 0.7\%$; RhoAWT - DC, $5.8 \pm 0.5\%$; RhoAV14 + DC, $5.8 \pm 0.5\%$; RhoAV14 + 5 pg/ml DC, $13.6 \pm 0.8\%$; RhoAN19 + DC, $6.3 \pm 0.6\%$; RhoAN19 - DC, $6.4 \pm 0.5\%$. Values for ligand remaining cell associated were as follows: RhoAWT + DC, $8.1 \pm 0.2\%$; RhoAWT - DC, $9.1 \pm 1.3\%$; RhoAV14 + DC, $5.7 \pm 1.0\%$; RhoAV14 + 5 pg/ml DC, $19.4 \pm 1.0\%$; RhoAN19 + DC, $2.5 \pm 0.2\%$; RhoAN19 - DC, $3.0 \pm 0.4\%$. Values (mean \pm SD; $n = 3$) are from a representative experiment. (A and C) ■, +DC, transcytosed; ●, +DC, recycled; ▲, -DC, transcytosed; ◆, -DC, recycled. (B) ■, +DC, transcytosed; ●, +DC, recycled; ▲, 5 pg/ml DC, transcytosed; ◆, 5 pg/ml DC, recycled.

cytosis was coupled with a large increase in the amount of ligand that recycled back to the basolateral pole of the cell ($\sim 10\%$ in control cells versus $\sim 40\%$ in cells expressing RhoAV14) (Figure 6B). Moreover, RhoAV14 expression resulted in an increase in the release of degraded ligand ($\sim 6\%$ in control cells versus 14% in cells expressing RhoAV14) and in the amount of ligand that remained cell associated ($\sim 6\%$ in control cells versus 19% in cells expressing RhoAV14). Expression of RhoAN19 did not alter the postendocytic fate of basolaterally internalized IgA (Figure 6C).

IgA Is Trapped at the Basolateral Pole of RhoAV14-expressing Cells

The large increase in basolateral recycling of IgA observed in RhoAV14-expressing cells is symptomatic of a block early in the transcytotic pathway. A similar phenotype is observed in pIgR-expressing cells treated with reagents that slow IgA exit from the basolateral early endosomes (e.g., nocodazole or cytochalasin D) (Breitfeld *et al.*, 1990; Hunziker *et al.*, 1990; Maples *et al.*, 1997). To determine if IgA was trapped in the basolateral early endosomes of RhoAV14-expressing cells, IgA was internalized for 10 min and the cells were washed and then chased for 5 min at 37°C. The cells were then processed for immunofluorescence, and the samples were examined by confocal microscopy. Figure 7 shows a series of optical sections (obtained with a confocal microscope) from the apical (A and E), lateral (B, C, F, and G), and basal (D and H) regions of the cell. In control cells (+DC), IgA was rapidly delivered to the apical pole of the cell, where it was found in punctate membrane structures (Figure 7, A and B). These structures have previously been characterized as elements of the common endosome/apical recycling endosome (Apodaca *et al.*, 1994; Barroso and Sztul, 1994; Odorizzi *et al.*, 1996). Less ligand was found along the lateral surfaces of the cells (Figure 7C) and at the base of the cells (Figure 7D).

In contrast, in RhoAV14-expressing cells, IgA was not concentrated at the apical pole of the cell (Figure 7E) but in vesicular elements at the base of the cell (Figure 7H). These IgA-labeled basal endosomes often appeared to be aligned in parallel rows that ran the width of the cell. As noted in Figure 1, J–M, RhoAV14 was found in a cytosolic distribution as well as in punctate structures. Some of the RhoAV14-labeled punctae at the base of the cells colocalized with IgA (Figure 8, A–C), indicating that these RhoAV14-positive structures were endosomal in nature. The other RhoAV14-positive punctate structures found in the lateral and apical cytoplasm did not colocalize with IgA, and their identity is unknown at present. Endogenous, wild-type RhoA had a similar intracellular distribution to that of RhoAV14 and was associated with numerous punctate structures in the cell cytoplasm, including those at the base of the cell, some of which colocalized with IgA (Figure 8, D–F). This observation indicates that a fraction of endogenous RhoA is normally associated with basolateral endosomes.

To determine if RhoAV14 expression resulted in the association of F-actin with the limiting membrane of basal endosomes, we colocalized IgA and F-actin with the use of confocal microscopy. At the very base of the cell, below the level of the stress fibers, a high degree of colocalization was observed between IgA and F-actin (Figure 9, C, F, and I). Small, punctate, F-actin-rich structures were also seen associated with, or sandwiched between, F-actin cables (Figure 9,

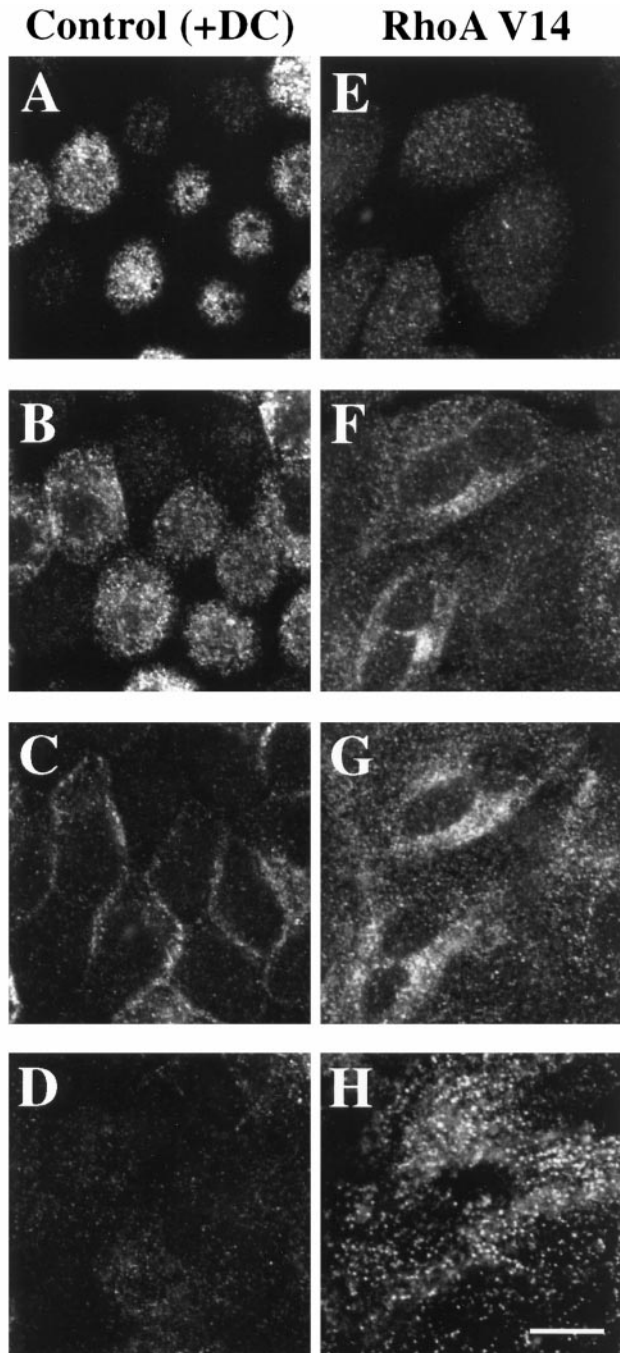


Figure 7. Distribution of basolaterally internalized IgA in RhoAV14 cells. RhoAV14 cells were grown in the presence of 20 ng/ml DC (A–D) or 5 pg/ml DC (E–H). IgA was internalized from the basolateral pole of the cell for 10 min at 37°C, and the cells were washed quickly and then chased in ligand-free medium for 5 min at 37°C. The cells were fixed with paraformaldehyde, incubated with rabbit anti-IgA antibody and a myc tag–specific mAb, and then reacted with fluorescently labeled secondary antibodies. Only staining for IgA is shown. Single optical sections, obtained with a confocal microscope, are shown from the base of the cell (D and H), the lateral surfaces of the cell at the level of the nucleus (C and G), 2 μ m above the previous section (B and F), and at the apex of the cell (A and E). Bar, 10 μ m.

B, E, and H). These F-actin–labeled punctate structures often colocalized with IgA, indicating that many of them were endosomal in nature (Figure 9, B, E, and H). However, we also observed IgA-labeled endosomes that were not actin positive and that appeared in the same optical plane in which the actin-labeled stress fibers appeared maximally in focus (Figure 9D). These IgA-containing endosomes often appeared to be aligned next to or sandwiched between adjacent F-actin–labeled stress fibers (Figure 9G). Similar results were obtained when F-actin was colocalized with basolaterally internalized Tf (our unpublished results). There was little colocalization of F-actin with IgA-labeled lateral and apical endosomes (our unpublished results).

To determine if the association of endosomes with F-actin was particular to cells expressing RhoAV14, we performed the same experiment with control cells (RhoAV14 cells grown in the presence of 20 ng/ml DC). In these experiments, IgA was internalized from the basolateral pole of the cell for 5 min at 37°C, and cell-surface ligand was removed by trypsin stripping before the samples were processed for confocal microscopy. The normal wash and chase after ligand internalization was omitted because, in control cells, IgA does not accumulate at the base of the cell and is rapidly delivered to the apical pole of the cell (Apodaca *et al.*, 1994). The distribution of IgA and F-actin was similar to what was observed in RhoAV14-expressing cells. However, as described previously, the amount of F-actin associated with stress fibers was decreased in these control cells (Jou and Nelson, 1998). IgA and F-actin were found to colocalize at the base of the cell (Figure 10, C, F, and I). In addition, there were F-actin–positive, IgA-labeled endosomes that were associated with or sandwiched between the F-actin–labeled stress fibers (Figure 10, B, E, and H). F-actin–negative but IgA-positive endosomes were also observed in a slightly higher plane of focus (Figure 10, A, D, and G). Often, these IgA-positive endosomes appeared in linear arrays.

Exit from Basolateral Endosomes Is Slow in RhoAV14-expressing MDCK Cells

The morphological analysis described above indicated that the significant slowing of IgA transcytosis in RhoAV14-expressing cells was in part the result of a defect in IgA movement toward the apical pole of the cell. To determine if this was the case, we used a previously described density-shift assay that measures the movement of IgA from the basal endosomes to apical endosomes loaded with an apically internalized marker conjugated to HRP (Apodaca *et al.*, 1994). [¹²⁵I]IgA was internalized basolaterally, whereas WGA-HRP was cointernalized from the apical pole of the cell for 10 min at 37°C. Ligand was removed from the cell surface, and the cells were treated with DAB and H₂O₂ to cross-link [¹²⁵I]IgA present in the WGA-HRP–filled apical endosome into a dense, detergent-insoluble complex that can be recovered by centrifugation. When normalized to the maximum amount of [¹²⁵I]IgA found in the apical endosomal compartment, we estimated that ~70% of [¹²⁵I]IgA internalized for 10 min at 37°C resides in an apical endosomal compartment of control cells (Figure 11). In contrast, in cells expressing RhoAV14, delivery of [¹²⁵I]IgA to these apical compartments was significantly inhibited by ~70% (Figure 11).

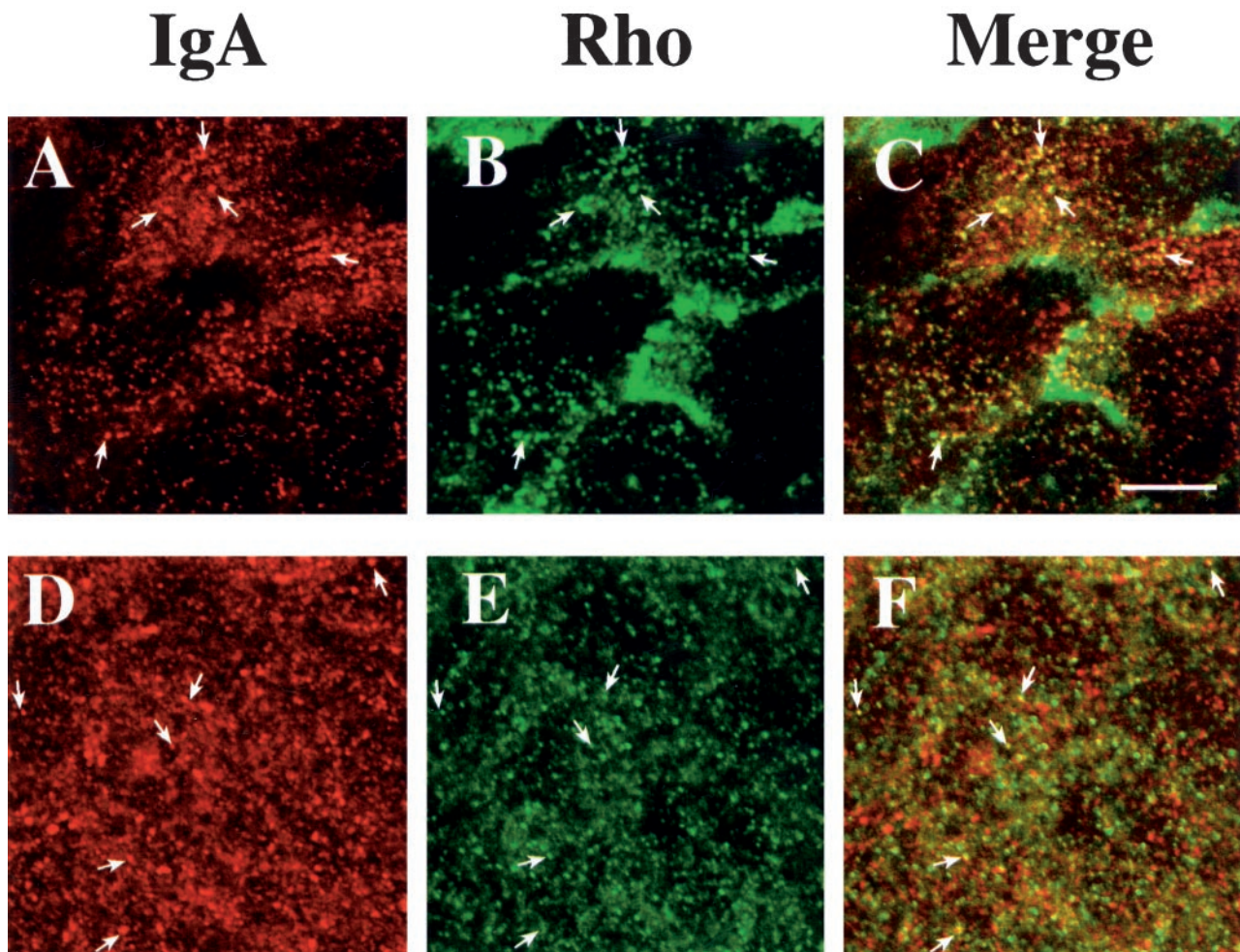


Figure 8. Distribution of basolaterally internalized IgA and endogenous RhoA or myc-tagged RhoAV14. RhoAV14 cells were grown in the presence of 5 pg/ml DC (A–C) or 20 ng/ml DC (D–F). IgA was internalized from the basolateral pole of the cell for 10 min at 37°C, and cell surface ligand was removed by chasing in ligand-free medium for 5 min at 37°C (A–C) or by trypsin treatment at 4°C (D–F). The cells were fixed with paraformaldehyde, incubated with rabbit anti-IgA antibody (A–F) and a myc tag-specific mAb (A–C) or a monoclonal anti-RhoA antibody (D–F), and then reacted with goat anti-rabbit Cy5 and goat anti-mouse FITC secondary antibodies. Panel A is identical to panel H in Figure 7, and panel B is identical to panel M in Figure 1. In the latter case, the contrast was enhanced and the image brightened to demonstrate colocalization of myc-tagged RhoAV14 and IgA. Examples of IgA and endogenous RhoA or myc-tagged RhoAV14 colocalization are marked with arrows. Bar, 10 μ m.

DISCUSSION

RhoA is known to regulate numerous cellular functions, including stress fiber formation, focal adhesion assembly, stimulation of MAPK cascades, phagocytosis, secretion, and receptor-mediated endocytosis (Van Aelst and D'Souza-Schorey, 1997; Hall, 1998). We now report that activation of RhoA can have multiple downstream consequences on several polarized cell membrane trafficking events, including apical and basolateral endocytosis, basolateral recycling, and transcytosis in the basolateral-to-apical direction.

Regulation of Apical and Basolateral Endocytosis by RhoA

There is increasing evidence that Rho family members may be important regulators of endocytosis. Mutant

RhoA and Rac1 alter fluid-phase as well as receptor-mediated endocytosis in nonpolarized cells (Ridley *et al.*, 1992; Schmalzing *et al.*, 1995; Lamaze *et al.*, 1996; Li *et al.*, 1997). Lamaze *et al.* (1996) reported that in HeLa cells, dominant active RhoA inhibits endocytosis and RhoA inactivation stimulates receptor-mediated endocytosis. In our current analysis, we observe that RhoA had the opposite effect; apical and basolateral endocytosis was accelerated in RhoAV14-expressing cells, whereas apical and basolateral endocytosis was inhibited in RhoAN19-expressing cells. These observations indicate that in polarized epithelial cells RhoA activation stimulates endocytosis, whereas RhoA inactivation inhibits endocytosis. The discrepancy between these two studies may reflect inherent differences in how nonpolarized and polarized

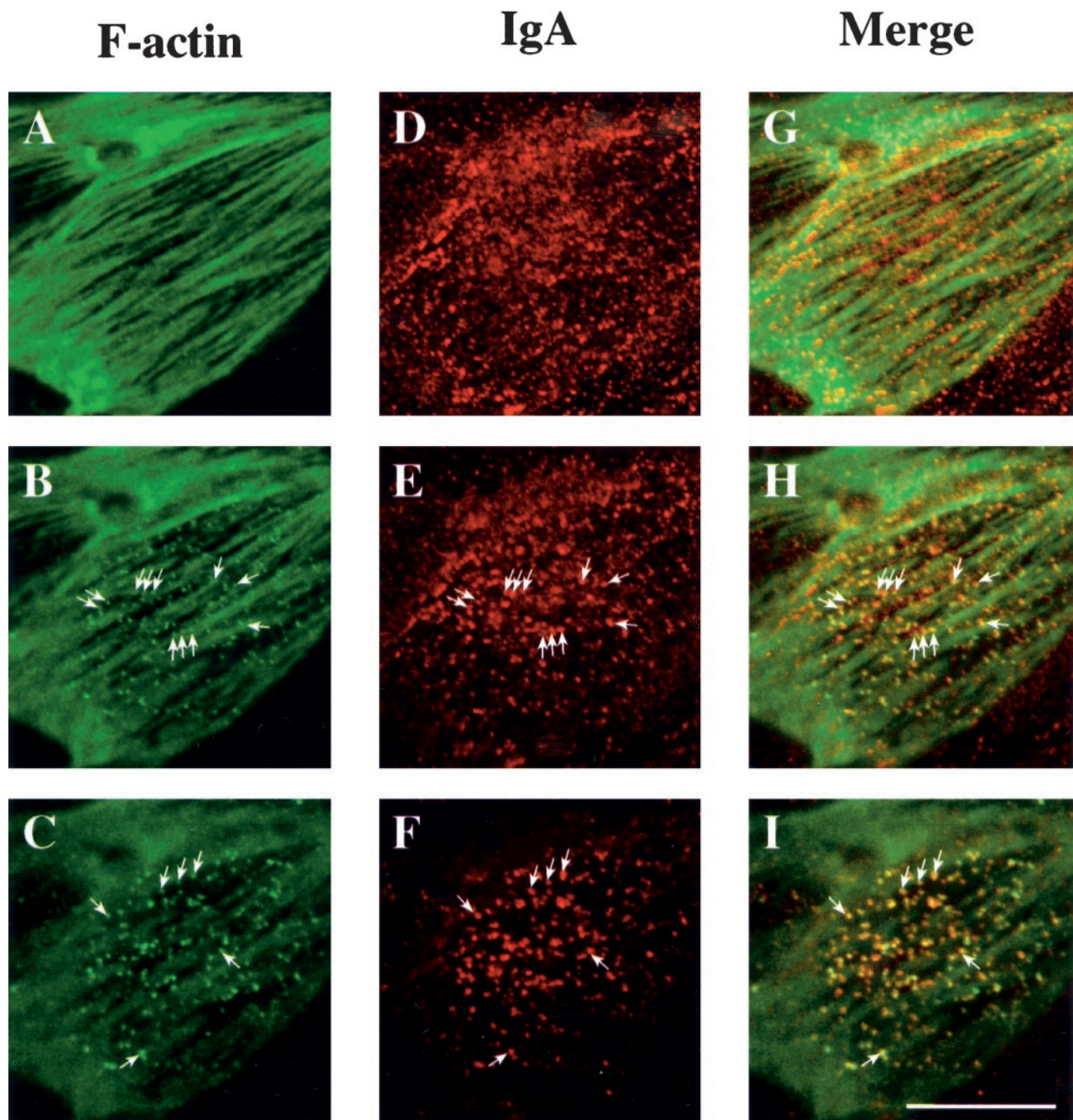


Figure 9. Distribution of IgA and F-actin in cells expressing RhoAV14. IgA was internalized for 10 min at 37°C from the basolateral surface of RhoAV14 cells grown in the presence of 5 pg/ml DC and then washed and chased for 5 min at 37°C. Cells were fixed with paraformaldehyde, incubated with rabbit anti-IgA antibody, and then reacted with goat anti-rabbit Cy5 secondary antibody and FITC-phalloidin. The FITC and Cy5 emissions were captured simultaneously with the use of a scanning laser confocal microscope. Single optical sections were taken at the very base of the cell (C, F, and I), 1 μm above the previous section (B, E, and H), and at a focal plane where the phalloidin-labeled stress fibers appeared maximally in focus (A, D, and G). Examples of IgA and F-actin colocalization are marked with arrows. Bar, 10 μm .

cells regulate endocytosis. We recently observed that a dominant active mutant of Rac1 (Rac1V12) decreases apical and basolateral endocytosis, whereas a dominant neg-

ative mutant (Rac1N19) stimulates endocytosis from both poles of the MDCK cell (Jou *et al.*, 2000). The opposing actions of Rac1 and RhoA suggest a mechanism whereby

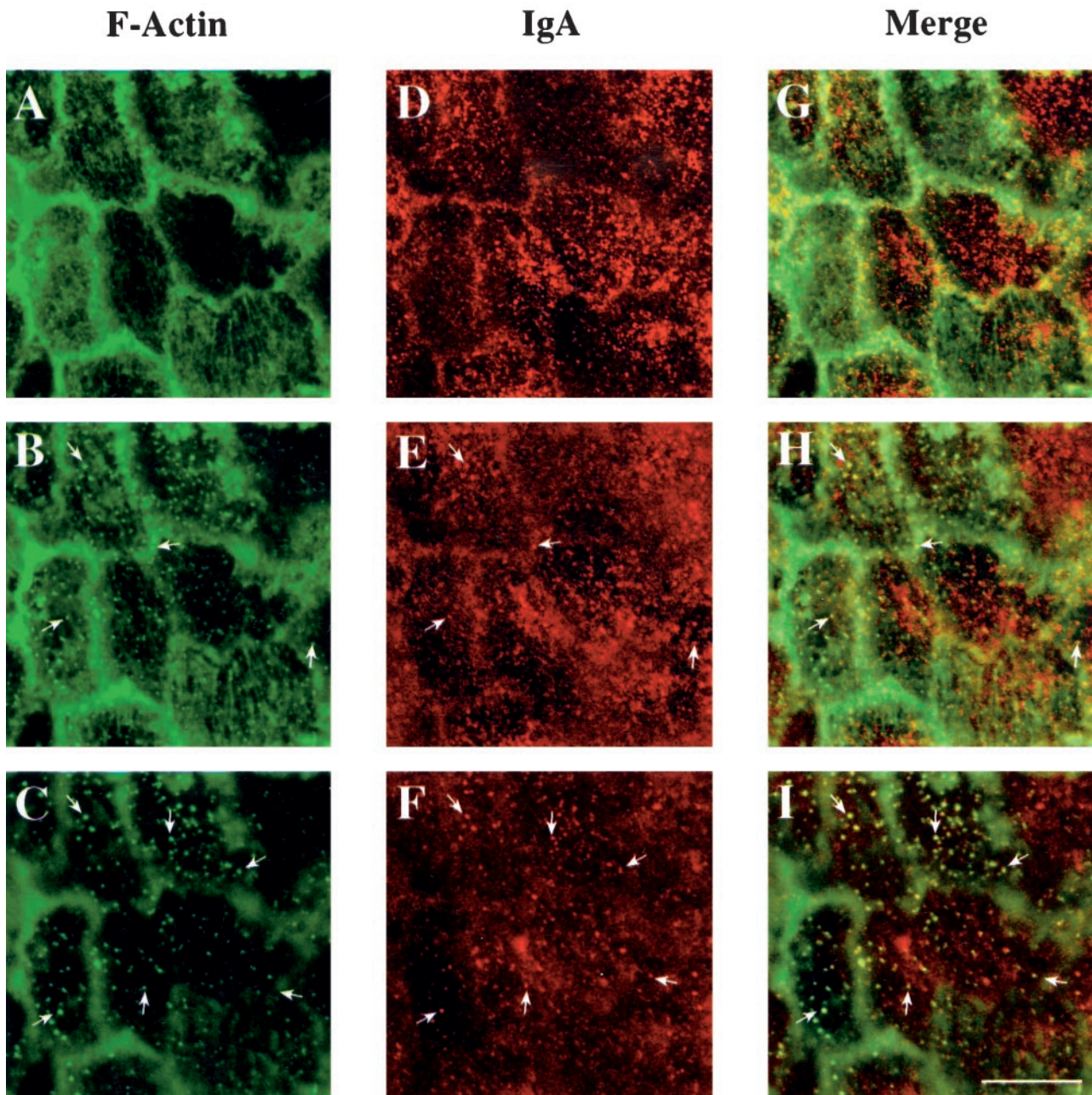


Figure 10. Distribution of IgA and F-actin in RhoAV14 grown in the presence of 20 ng/ml DC. IgA was internalized for 10 min at 37°C from the basolateral surface of RhoAV14 cells grown in the presence of 20 ng/ml DC, and the cell surface ligand was removed by trypsin treatment at 4°C. Cells were fixed with paraformaldehyde, incubated with rabbit anti-IgA antibody, and then reacted with goat anti-rabbit Cy5 secondary antibody and FITC-phalloidin. The FITC and Cy5 emissions were captured simultaneously with the use of a scanning laser confocal microscope. Single optical sections were taken at the very base of the cell (C, F, and I), 1 μm above the previous section (B, E, and H), and at a focal plane where the phalloidin-labeled stress fibers appeared maximally in focus (A, D, and G). Examples of IgA and F-actin colocalization are marked with arrows. Bar, 10 μm .

different extracellular cues could differentially regulate endocytosis in polarized epithelial cells; agents that signal through Rac1 (e.g., the insulin receptor or EGF receptor)

would inhibit endocytosis, whereas activation of RhoA (e.g., via the lysophosphatidic acid receptor) could lead to increases in receptor-mediated endocytosis.

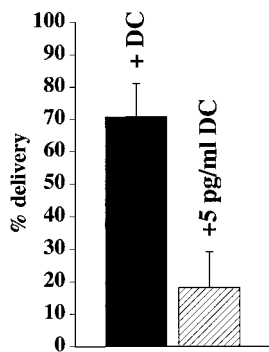


Figure 11. Quantification of IgA delivery to apical endosomes in RhoAV14 cells. [125 I]IgA was internalized basolaterally for 10 min at 37°C, whereas WGA-HRP was cointernalized from the apical surface of RhoAV14 cells grown in the presence of 20 ng/ml DC (+DC) or 5 pg/ml DC (+5 pg/ml DC). Details of the DAB reaction and quantitation are given in MATERIALS AND METHODS. Values (mean \pm SD; $n = 3$) are from a representative experiment.

RhoAV14 Primarily Alters Postendocytic Traffic at the Basolateral Pole of MDCK Cells

Although there have been several reports of Rho family members regulating endocytosis and exocytosis (reviewed by Van Aelst and D'Souza-Schorey, 1997), little is known about the roles of these proteins in postendocytic or biosynthetic traffic. We recently observed in Rac1V12-expressing cells that apically directed membrane traffic is more severely impaired than traffic directed toward the basolateral pole of the cell (Jou *et al.*, 2000). This inhibition was largely the result of trapping of endocytosed markers in a central membranous aggregate.

In contrast, we observed here that RhoAV14 expression had little effect on apical recycling of IgA. Instead, RhoAV14 primarily altered basolateral recycling of Tf, slowed degradation of basolaterally internalized EGF, and inhibited basolateral-to-apical transcytosis of IgA. Tf recycling was markedly slowed, and there was a large increase (threefold) in the amount of Tf ligand released from the apical pole of the cell. The increase in Tf transcytosis was surprising because transcytosis of basolaterally internalized IgA was severely impaired in RhoAV14-expressing cells. Moreover, we observed that significant amounts of Tf were retained in basal endosomes (Leung, unpublished observations), although some Tf was also observed in the apical cytoplasm of these cells. Overexpression of RhoAV14 may alter the normally efficient basolateral sorting/targeting machinery in endosomes and/or at the basolateral cell surface, resulting in apical release of Tf ligand from, most likely, the apically distributed endosomal elements. The increase in Tf release at the apical pole of the cell was not simply a result of paracellular diffusion, because we cultured cells under conditions in which RhoAV14-mediated changes in tight junction formation were moderate.

Degradation of basolaterally internalized EGF was also slowed by RhoAV14 expression. However, this was primarily a kinetic effect, because inhibition of EGF degradation was only 15%, which may reflect alterations in basal endosome function (see below). The largest effect of RhoAV14 expression was a 70% inhibition of basolateral-to-apical transcytosis of IgA. This was coupled with a significant increase in the amount of IgA that was released at the basolateral pole of the cell. As described below, alterations in basolateral endosome dynamics may explain some of these defects in transcytosis.

Although RhoAV14 expression altered postendocytic traffic, expression of RhoAN19 or RhoAWT had little effect on

these trafficking pathways. This was unexpected, because RhoAN19 expression inhibited endocytosis and one might predict that RhoAN19 expression would alter postendocytic traffic. This lack of effect may be the result of poor RhoAN19 expression. Experimentally, it has been challenging to generate stable cell lines that express dominant negative forms of RhoA (Takaishi *et al.*, 1997; Jou and Nelson, 1998). Although this level of RhoAN19 expression was sufficient to decrease transepithelial resistance and to inhibit endocytosis (Jou and Nelson, 1998; Jou *et al.*, 1998; this study), it may be insufficient to alter postendocytic traffic. Other systems have been described in which only the dominant active forms of small GTPases (e.g., Rab25 and Rac1) have effects on postendocytic traffic (Casanova *et al.*, 1999; Jou *et al.*, 2000). Perhaps these trafficking pathways respond only to the activation of these particular small GTPases. An alternative possibility is that RhoA is not absolutely required for normal postendocytic traffic to occur. However, the presence of endogenous RhoA on a subpopulation of basolateral endosomes might suggest otherwise. Additionally, failure to observe an effect with a dominant negative mutant does not rule out involvement of the wild-type protein. Ras activity can be induced directly by nitric oxide and can be modulated by decreases in the activity of guanine nucleotide exchange factors (Downward *et al.*, 1990; Mott *et al.*, 1997). As noted previously, neither of these mechanisms of Ras activation would be sensitive to expression of a dominant negative mutant (Feig, 1999).

The Transcytotic Pathway Is Blocked at an Early Step in RhoAV14-expressing Cells

The significant decrease in transcytosis of basolaterally internalized IgA may reflect altered endosomal function and dynamics at the base of the RhoAV14-expressing cells. Normally, transcytosing IgA moves rapidly from the basolateral early endosomes to the apical pole of cells, where it mixes with apically internalized membrane cargo (Apodaca *et al.*, 1994). We have measured this translocation step in RhoAV14-expressing cells and found that it was significantly slowed. Although this slowing could reflect an inhibition of fusion between basolateral and apical cargo, we observed that in RhoAV14-expressing cells a significant fraction of the internalized IgA was found in basal endosomes. Moreover, myc-tagged RhoAV14 was localized to these basolateral endosomes, and F-actin was found associated with the limiting membrane of these endosomes.

The association of F-actin and RhoA with basolateral endosomes was not particular to cells expressing RhoAV14; it was also observed in control cells. These results indicate that a fraction of endogenous RhoA is normally associated with a subpopulation of basolateral endosomes and therefore could regulate the function/dynamics of these endosomes. RhoA, for example, could be important in modulating the actin cytoskeleton and/or the association of myosin motors with these basolateral endosomes. In fact, there is evidence that an unconventional myosin motor (Myr5) contains a GTPase-activating domain for RhoA (Reinhard *et al.*, 1995). In some respects, RhoA functions like RhoD. This member of the Rho family is associated with endosomes. In cells expressing a dominant active mutant of RhoD (RhoD^{G26V}), the endosomes lack tubular extensions, lose their dynamic properties, are associated with actin, and often appear in linear

arrays (Murphy *et al.*, 1996). Unlike RhoAV14-expressing cells, cells expressing RhoD^{G26V} have only a minimal effect on the internalization and recycling of Tf. A dominant negative mutant of RhoD (RhoD^{T31N}) has no observable effects on the actin cytoskeleton or endosome dynamics/function. This lack of effect is consistent with our observation that RhoAN19 did not alter postendocytic traffic.

In addition to its ability to modulate the actin cytoskeleton, RhoA is known to activate multiple downstream effectors, including phospholipase D, phosphoinositol-4-phosphate-5-kinase, ROK α /Rho kinase, p160 ROCK, p140mDia, PKN, Rhotekin, RhoGAP, and citron (reviewed by Van Aelst and D'Souza-Schorey, 1997; Mackay and Hall, 1998). Although many of these effectors are known to induce changes in the actin cytoskeleton, phospholipase D and phosphoinositol-4-phosphate-5-kinase have the additional effect of controlling coat binding to organellar membranes (Liscovitch and Cantley, 1995; De Camilli *et al.*, 1996; Liscovitch, 1996). As such, the efficient formation or inclusion of cargo into vesicles involved in postendocytic traffic could be altered by RhoAV14. Perhaps the coats that recognize basolateral targeting information are disrupted in cells expressing RhoAV14, and as a result, depolarized secretion of Tf occurs. In addition to potential defects in endosome/actin interactions, alterations in coat binding may also play a role in producing the large inhibition of transcytosis observed in RhoAV14-expressing cells. We are currently exploring the role of these various Rho effectors on postendocytic traffic.

In summary, our observations indicate that RhoA may have a previously unappreciated role in modulating endocytic traffic in polarized MDCK cells. These findings are relevant not only in understanding normal cellular physiology but also in conditions in which normal cellular function is altered. Rho family members have been implicated in cancer progression, and of the more than 20 guanine nucleotide exchange factors for members of the Rho family, all of them are potentially oncogenic, presumably as a result of their uncontrolled activation of Rho family members (Qiu *et al.*, 1995; Olson, 1996; Van Aelst and D'Souza-Schorey, 1997; Vojtek and Der, 1998). Uncontrolled RhoA activation, therefore, could lead to disruption of membrane traffic, loss of cell polarity, and progression into a malignant phenotype.

ACKNOWLEDGMENTS

We thank Dr. W.J. Nelson for his insightful comments and critiques during the preparation of the manuscript. This work was supported by grant RO1DK51970 from the National Institutes of Health to G.A. The Laboratory of Epithelial Cell Biology is supported in part by a grant from Dialysis Clinics, Inc.

REFERENCES

Adam, T., Giry, M., Boquet, P., and Sansonetti, P. (1996). Rho-dependent membrane folding causes *Shigella* entry into epithelial cells. *EMBO J.* 15, 3315–3321.

Adamson, P., Paterson, H.F., and Hall, A. (1992). Intracellular localization of the p21^{ras} proteins. *J. Cell Biol.* 119, 617–627.

Apodaca, G., Bomsel, M., Arden, J., Breitfeld, P.P., Tang, K., and Mostov, K.E. (1991). The polymeric immunoglobulin receptor: a model protein to study transcytosis. *J. Clin. Invest.* 87, 1877–1882.

Apodaca, G., Cardone, M.H., Whiteheart, S.W., DasGupta, B.R., and Mostov, K.E. (1996). Reconstitution of transcytosis in SLO-permeabilized MDCK cells: existence of an NSF dependent fusion mechanism with the apical surface of MDCK cells. *EMBO J.* 15, 1471–1481.

Apodaca, G., Katz, L.A., and Mostov, K.E. (1994). Receptor-mediated transcytosis of IgA in MDCK cells is via apical recycling endosomes. *J. Cell Biol.* 125, 67–86.

Barroso, M., and Sztul, E. (1994). Basolateral to apical transcytosis in polarized cells is indirect and involves BFA and trimeric G protein sensitive passage through the apical endosome. *J. Cell Biol.* 124, 83–100.

Barth, A.I., Pollack, A.L., Altschuler, Y., Mostov, K.E., and Nelson, W.J. (1997). NH₂-terminal deletion of beta-catenin results in stable colocalization of mutant beta-catenin with adenomatous polyposis coli protein and altered MDCK cell adhesion. *J. Cell Biol.* 136, 693–706.

Bomsel, M., Parton, R., Kuznetsov, S.A., Schroer, T.A., and Gruenberg, J. (1990). Microtubule- and motor-dependent fusion in vitro between apical and basolateral endocytic vesicles from MDCK cells. *Cell* 62, 719–731.

Brandli, A.W., Adamson, E.D., and Simons, K. (1991). Transcytosis of epidermal growth factor: the epidermal growth factor receptor mediates uptake but not transcytosis. *J. Biol. Chem.* 266, 8560–8566.

Breitfeld, P., Casanova, J.E., Harris, J.M., Simister, N.E., and Mostov, K.E. (1989a). Expression and analysis of the polymeric immunoglobulin receptor. *Methods Cell Biol.* 32, 329–337.

Breitfeld, P.P., Harris, J.M., and Mostov, K.M. (1989b). Postendocytotic sorting of the ligand for the polymeric immunoglobulin receptor in Madin-Darby canine kidney cells. *J. Cell Biol.* 109, 475–486.

Breitfeld, P.P., McKinnon, W.C., and Mostov, K.E. (1990). Effect of nocodazole on vesicular traffic to the apical and basolateral surfaces of polarized MDCK cells. *J. Cell Biol.* 111, 2365–2373.

Casanova, J.E., Wang, X., Kumar, R., Bhartur, S.G., Navarre, J., Woodrum, J.E., Altschuler, Y.A., Ray, G.S., and Godenring, J.R. (1999). Association of Rab25 and Rab11a with the apical recycling system of polarized Madin-Darby canine kidney cells. *Mol. Biol. Cell* 10, 47–61.

Chen, L.-M., Hobbie, S., and Galán, J.E. (1996). Requirement of CDC42 for *Salmonella*-induced cytoskeletal and nuclear responses. *Science* 274, 2115–2118.

Cussac, D., Leblanc, P., L'Heritier, A., Bertoglio, J., Lang, P., Kordon, C., Enjalbert, A., and Saltarelli, D. (1996). Rho proteins are localized with different membrane compartments involved in vesicular trafficking in anterior pituitary cells. *Mol. Cell. Endocrinol.* 119, 195–206.

De Camilli, P., Emr, S.D., McPherson, P.S., and Novick, P. (1996). Phosphoinositides as regulators in membrane traffic. *Science* 271, 1533–1539.

Downward, J., Graves, J.D., Warne, P.H., Rayter, S., and Cantrell, D.A. (1990). Stimulation of p21ras upon T-cell activation. *Nature* 346, 719–723.

Durrbach, A., Louvard, D., and Coudrier, E. (1996). Actin filaments facilitate two steps of endocytosis. *J. Cell Sci.* 109, 457–465.

Feig, L.A. (1999). Tools of the trade: use of dominant-inhibitory mutants of Ras-family GTPases. *Nat. Cell Biol.* 1, E25–E27.

Fuller, S.D., and Simons, K. (1986). Transferrin receptor polarity and recycling accuracy in "tight" and "leaky" strains of Madin-Darby canine kidney cells. *J. Cell Biol.* 103, 1767–1779.

Geli, M.I., and Riezman, H. (1996). Role of type I myosins in receptor-mediated endocytosis in yeast. *Science* 272, 533–535.

- Gottlieb, T.A., Ivanov, I.E., Adesnik, M., and Sabatini, D.D. (1993). Actin microfilaments play a critical role in endocytosis at the apical but not the basolateral surface of polarized epithelial cells. *J. Cell Biol.* *120*, 695–710.
- Grindstaff, K.K., Bacallao, R.L., and Nelson, W.J. (1998). Apionuclear organization of microtubules does not specify protein delivery from the trans-Golgi network to different membrane domains in polarized epithelial cells. *Mol. Biol. Cell* *9*, 685–699.
- Gruenberg, J., Griffiths, G., and Howell, K. (1989). Characterization of the early endosome and putative endocytic carrier vesicles in vivo and with an assay of vesicle fusion in vitro. *J. Cell Biol.* *108*, 1301–1316.
- Hall, A. (1998). Rho GTPases and the actin cytoskeleton. *Science* *279*, 509–514.
- Hunziker, W., Mâle, P., and Mellman, I. (1990). Differential microtubule requirements for transcytosis in MDCK cells. *EMBO J.* *9*, 3515–3525.
- Jackman, M.R., Shurety, W., Ellis, J.A., and Luzio, J.P. (1994). Inhibition of apical but not basolateral endocytosis of ricin and folate in Caco-2 cells by cytochalasin D. *J. Cell Sci.* *107*, 2547–2556.
- Jou, T.-S., Leung, S.-M., Fung, L.M., Ruiz, W.G., Nelson, W.J., and Apodaca, G. (2000). Selective alterations in the biosynthetic and endocytic protein traffic in MDCK epithelial cells expressing mutants of the small GTPase RAC1. *Mol. Biol. Cell* (*in press*).
- Jou, T.-S., and Nelson, W.J. (1998). Effects of regulated expression of mutant RhoA and Rac1 small GTPases on the development of epithelial (MDCK) cell polarity. *J. Cell Biol.* *142*, 85–100.
- Jou, T.-S., Schneeberger, E.E., and Nelson, W.J. (1998). Structural and functional regulation of tight junctions by RhoA and Rac1 small GTPases. *J. Cell Biol.* *142*, 101–115.
- Kozma, R., Ahmed, S., Best, A., and Lim, L. (1995). The Ras-related protein Cdc42Hs and bradykinin promote formation of peripheral actin microspikes and filopodia in Swiss 3T3 fibroblasts. *Mol. Cell Biol.* *15*, 1942–1952.
- Kroschewski, R., Hall, A., and Mellman, I. (1999). Cdc42 controls secretory and endocytic transport to the basolateral plasma membrane of MDCK cells. *Nat. Cell Biol.* *1*, 8–13.
- Kübler, E., and Riezman, H. (1993). Actin and fimbrin are required for the internalization step of endocytosis in yeast. *EMBO J.* *12*, 2855–2862.
- Lamaze, C., Chuang, T.-H., Terlecky, L.J., Bokoch, G.M., and Schmid, S.L. (1996). Regulation of receptor-mediated endocytosis by Rho and Rac. *Nature* *382*, 177–179.
- Lamaze, C., Fujimoto, L.M., Yin, H.L., and Schmid, S.L. (1997). The actin cytoskeleton is required for receptor-mediated endocytosis in mammalian cells. *J. Biol. Chem.* *272*, 20332–20335.
- Li, G., D'Souza-Schorey, C., Barbieri, M.A., Cooper, J.A., and Stahl, P.D. (1997). Uncoupling of membrane ruffling and pinocytosis during ras signal transduction. *J. Biol. Chem.* *272*, 10337–10340.
- Liscovitch, M. (1996). Phospholipase D: role in signal transduction and membrane traffic. *J. Lipid Mediators Cell Signal.* *14*, 215–221.
- Liscovitch, M., and Cantley, L.C. (1995). Signal transduction and membrane traffic: the P1TP/phosphoinositide connection. *Cell* *81*, 659–662.
- Mackay, D.J.G., and Hall, A. (1998). Rho GTPases. *J. Biol. Chem.* *273*, 20685–20688.
- Maples, C.J., Ruiz, W.G., and Apodaca, G. (1997). Both microtubules and actin filaments are required for efficient postendocytic traffic of the polymeric immunoglobulin receptor in polarized Madin-Darby canine kidney cells. *J. Biol. Chem.* *272*, 6741–6751.
- McGraw, T.E., Dunn, K.W., and Maxfield, F.R. (1993). Isolation of a temperature-sensitive variant Chinese hamster ovary cell line with a morphologically altered endocytic recycling compartment. *J. Cell Physiol.* *155*, 579–594.
- Mostov, K.E., and Cardone, M.H. (1995). Regulation of protein traffic in polarized epithelial cells. *BioEssays* *17*, 129–138.
- Mott, H.R., Carpenter, J.W., and Campbell, S.L. (1997). Structural and functional analysis of a mutant Ras protein that is insensitive to nitric oxide activation. *Biochemistry* *36*, 3640–3644.
- Mukherjee, S., Ghosh, R.N., and Maxfield, F.R. (1997). Endocytosis. *Physiol. Rev.* *77*, 759–803.
- Murphy, C., Saffrich, R., Grummt, M., Gournier, H., Rybin, V., Rubino, M., Auvinen, P., Lütcke, A., Parton, R.G., and Zerial, M. (1996). Endosome dynamics regulated by a Rho protein. *Nature* *384*, 427–432.
- Odorizzi, G., Pearse, A., Domingo, D., Trowbridge, I.S., and Hopkins, C.R. (1996). Apical and basolateral endosomes of MDCK cells are interconnected and contain a polarized sorting mechanism. *J. Cell Biol.* *135*, 139–152.
- Olson, M.F. (1996). Guanine nucleotide exchange factors for the Rho GTPases: a role in human disease? *J. Mol. Med.* *74*, 563–571.
- Qiu, R.-G., Chen, J., McCormick, F., and Symons, M. (1995). A role for Rho in Ras transformation. *Proc. Natl. Acad. Sci. USA* *92*, 11781–11785.
- Reinhard, J., Scheel, A.A., Diekmann, D., Hall, A., Ruppert, C., and Bahler, M. (1995). A novel type of myosin implicated in signaling by rho family GTPases. *EMBO J.* *14*, 697–704.
- Ridley, A.J., and Hall, A. (1992). The small GTP-binding protein Rho regulates the assembly of focal adhesions and actin stress fibers in response to growth factors. *Cell* *70*, 389–399.
- Ridley, A.J., Paterson, H.F., Johnston, C.L., Diekmann, D., and Hall, A. (1992). The small GTP-binding protein rac regulates growth factor-induced membrane ruffling. *Cell* *70*, 401–410.
- Schmalzing, G., Richter, H.-P., Hansen, A., Schwarz, W., Just, I., and Aktories, K. (1995). Involvement of the GTP binding protein Rho in constitutive endocytosis in *Xenopus laevis* oocytes. *J. Cell Biol.* *130*, 1319–1332.
- Schmid, S.L. (1997). Clathrin-coated vesicle formation and protein sorting: an integrated process. *Annu. Rev. Biochem.* *66*, 511–548.
- Takaishi, K., Sasaki, T., Kotani, H., Nishioka, H., and Takai, Y. (1997). Regulation of cell-cell adhesion by Rac and Rho small G proteins in MDCK cells. *J. Cell Biol.* *139*, 1047–1059.
- Urban, J., Parczyk, K., Leutz, A., Kayne, M., and Kondor-Koch, C. (1987). Constitutive apical secretion of an 80-kDa sulfated glycoprotein complex in the polarized epithelial Madin-Darby canine kidney cell line. *J. Cell Biol.* *105*, 2735–2743.
- Van Aelst, L., and D'Souza-Schorey, C. (1997). Rho GTPases and signaling networks. *Genes Dev.* *11*, 2295–2322.
- Vojtek, A.B., and Cooper, J.A. (1995). Rho family members: activators of MAP kinase cascades. *Cell* *82*, 527–529.
- Vojtek, A.B., and Der, C.J. (1998). Increasing complexity of the ras signaling pathway. *J. Biol. Chem.* *273*, 19925–19928.
- Watarai, M., Kamata, Y., Kozaki, S., and Sasakawa, C. (1997). Rho, a small GTP-binding protein, is essential for *Shigella* invasion of epithelial cells. *J. Exp. Med.* *185*, 281–292.